

International Journal of Control Theory and Applications

ISSN : 0974-5572

© International Science Press

Volume 9 • Number 50 • 2016

Analysis and Mitigation of Interharmonics in Variable Frequency Drive with Motor Current Unbalance

D. Uma and K. Vijayarekha

Department of Electrical and Electronics Engineering SASTRA University, Thanjavur, Tamilnadu-613 401, India
E-mail: umavijay@eee.sastra.edu

Abstract: Harmonic and Interharmonic distortions seriously affect the normal functioning of the power system. These distortions are caused by the use of power electronic converters such as rectifiers and inverters. Particularly a Variable Frequency Drive (VFD) with rectifier, dc link and an inverter fed induction motor introduces harmonic and interharmonic distortions both in supply side and load side. In this work analysis is made for the propagation of interharmonics from unbalanced motor load to the supply side. Different mitigation methods are suggested to minimise harmonics and interharmonics in the input side of VFD. These methods are simulated in MATLAB/Simulink and the results are compared.

Keywords: Variable Frequency Drive, Interharmonics, Active filter, Passive filter, Harmonics

1. INTRODUCTION

Power electronic converters have been widely used in industries. Because of its wide spread use, quality of the power supplied to the customer is affected.

Interharmonics are components that are observed in power frequency voltages and currents which are non integer multiples of the fundamental frequency. They can appear as discrete frequencies or as a wide band spectrum [1]. In literature, the causes and effects of Interharmonics are discussed in detail [2-9]. Interharmonic components are generated when two systems with different frequencies are interconnected. In variable frequency drive, supply and motor are operating at different frequencies as they are interconnected by static frequency changer [10-11]. Here the static frequency changer consists of a three phase rectifier, dc link and three phase pulse width modulated voltage source inverter. Also, interharmonics are generated in the input side of the rectifier when the inverter output is in unbalanced condition [12-13] or it is operated in overmodulation. Also the presence of large capacitance in the dc link increases the disturbance in the input current of the rectifier [12]. In literature, a choke is used in the input side to mitigate interharmonics generated due to motor current imbalance [12]. But this will not reduce the harmonic components in the supply current and therefore THD of the supply current is more. This necessitates the requirement of a suitable method to reduce harmonics and interharmonics in the input current of the VFD. Moreover, in literature, importance is not given to supply voltage THD and load

voltage THD. Also, in literature for the analysis of harmonics and interharmonics, an accurate model is not derived mathematically. In this work, an accurate model for induction motor is developed using d-q reference frame equations and the same is used for analysis.

In this work, methods are suggested to reduce both harmonics and interharmonics in the supply. An AC-DC-AC converter fed induction motor is considered. Motor current imbalance is provided by connecting an inductor in series with phase B of the motor. This motor current imbalance results in motor current distortion. This propagates distortions into the inverter input current, thereby resulting in interharmonics in the input current of the rectifier. A detailed analysis is carried out in the propagation of distortion from motor side to the rectifier input side. This analysis is proven by simulation results. To damp out the distortions, first an inductor of approximate value is designed and simulation is carried out in MATLAB/Simulink. Then a passive filter is designed and its effectiveness is illustrated by simulation results. Distortion in the rectifier input current is further minimised by connecting a shunt active filter in the supply side. It is illustrated from the simulation results. Supply voltage THD and load voltage THD are also analysed for all the methods mentioned above.

2. ANALYSIS OF INTERHARMONICS GENERATION IN THE RECTIFIER INPUT

The block diagram of the system considered is shown in Fig. 1

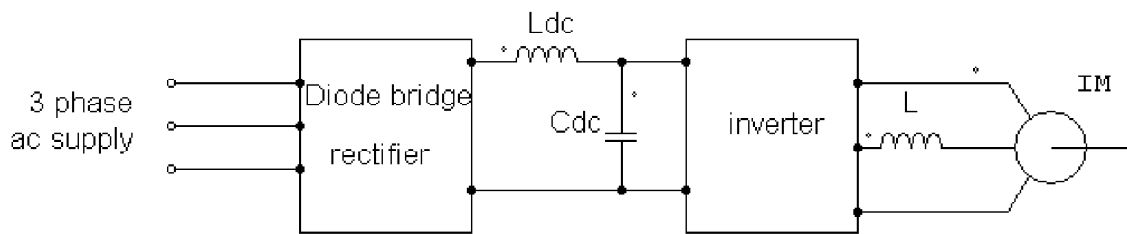


Figure 1

Three phase AC is converted into DC by using the front end converter. Then this DC is converted into AC by using a pulse width modulated inverter. The output of which is fed to an induction motor. An inductor is connected in series with one of the phase windings to emulate load unbalance. Then propagation of harmonics from load to the source is analysed.

3. PROPAGATION OF HARMONICS FROM MOTOR SIDE TO DC LINK

Pulse width modulation technique is used to obtain the output voltage from the inverter at the desired frequency. The output voltages of the inverter is given as

$$V_{uo} = \frac{V_{dc}}{2} (1 + m_i \cos \omega t) = V_{dc} S_{ui} \quad (1)$$

Where m_i is the modulation index and S_{ui} is the inverter switching function.

The inverter output voltages V_{vo} and V_{wo} are phase displaced by 120° and 240° respectively.

The switching function of the inverter is given by,

$$S_{ui} = \frac{1}{2} (m_i + \cos \omega t) \quad (2)$$

The switching functions S_{vi} and S_{wi} are phase shifted by 120° and 240° respectively.

The motor current is made unbalance by connecting an inductor in series with one of the phase windings. Due to this unbalance, in addition to positive sequence components, negative sequence components are also present in the motor current. The motor input current is given by,

$$i_{um} = \sqrt{2}I_p \cos(\omega t + \phi_p) + \sqrt{2}I_n \cos(\omega t + \phi_n) \quad (3)$$

Where, I_p -positive sequence component of current

I_n - negative sequence component of current

These current components have a phase shift of Φ_p and Φ_n .

Similarly phase v and phase w current equations can be obtained.

The inverter input current is obtained from the following equation

$$i_{dc} = S_{ui}i_{um} + S_{vi}i_{vm} + S_{wi}i_{wm} \quad (4)$$

$$S_{ui}i_{um} = \frac{1}{2}(1 + m_i \cos \omega t) \left[\left(\sqrt{2}(I_p) \cos(\omega t + \phi_p) \right) + \left(\sqrt{2}(I_n) \cos(\omega t + \phi_n) \right) \right] \quad (5)$$

Similarly expressions for $S_{vi}i_{vm}$ and $S_{wi}i_{wm}$ can be derived. After deriving these expressions, they are substituted in equation (4) to obtain i_{dc}

$$i_{dc} = \left(\frac{3}{4} m_i \sqrt{2} I_p \cos \phi_p \right) + \left(\frac{3}{2\sqrt{2}} m_i I_n \cos(2\omega_{out} t + \phi_n) \right) \quad (6)$$

$$i_{dc} = I_{dc} + I_{dist} \quad (7)$$

$$I_{dc} = \frac{3}{4} m_i \sqrt{2} I_p \cos \phi_p$$

Where

$$I_{dist} = \frac{3}{2\sqrt{2}} m_i I_n \cos(2\omega_{out} t + \phi_n) \quad (8)$$

I_{dc} – Positive sequence component responsible for active power transfer

I_{dist} – Negative sequence component responsible for disturbance in the inverter dc side current.

From equation (6), it is clear that the current i_{dc} fluctuates at two times the output frequency ω_{out} which is the operating frequency of the inverter.

4. CURRENT MAGNIFICATION IN THE DC LINK

The disturbance component present in the current i_{dc} excites parallel LC components in the dc link. Due to this, current magnification occurs near parallel resonance point. The disturbance current transferred to the rectifier and the rectifier current in the dc link is given by,

$$i_{rect} = I_{dc} + \sqrt{2} I_{rect} \cos(2\omega_{out} t + \phi) \quad (9)$$

Where

$$I_{rect} = k_{dclink} I_{dist} \quad (10)$$

$k_{dc\text{link}}$ is the current magnification factor in the dc link at the frequency $2f_{out}$ is given by

$$k_{dc\text{link}} = \left| \frac{R_c + C_{dc}}{(R_c + C_{dc}) + (R_L + L_{dc})} \right| \quad (11)$$

R_c and C_{dc} – Resistance and capacitance of the capacitor in the dc link

R_L and L_{dc} – Resistance and inductance of the inductor in the dc link

And
$$\phi = \phi_n + \phi_Z \quad (12)$$

Where ϕ_Z is the phase shift due to dc link.

When $[(R_c + C_{dc}) + R_L + L_{dc}]$ is equal to zero, large magnification of the inverter current takes place and large currents can appear in the rectifier side. The frequency corresponding to this condition is the parallel resonance frequency in the dc link and it is shown as,

$$f_{res} = \frac{1}{2\pi\sqrt{L_{dc} + C_{dc}}} \quad (13)$$

From equation (9) it can be concluded that if the inverter is operated in the frequency range $0-f_{out}$, then the rectifier side dc link current is increased considerably if the dc link resonance frequency is in the range $0-2f_{out}$.

5. PROPAGATION OF HARMONICS FROM RECTIFIER DC LINK SIDE TO THE RECTIFIER INPUT SIDE

In order to explain this, the switching functions of the rectifier are considered. Also it is assumed that the rectifier conducts continuously. Using this the rectifier input current is derived and is given by,

$$i_{ar} = S_{ar} i_{rect} \quad (14)$$

Where S_{ar} – switching function of the rectifier and is shown below

$$S_{ar} = A_1 \cos \omega_s t \quad (15)$$

Where A_1 is the amplitude of the fundamental component and it is equal to $\frac{2\sqrt{3}}{\pi}$ and ω_s is the supply frequency.

Similarly expressions for S_{br} and S_{cr} can be obtained that are phase shifted by 120° and 240° respectively. Further the rectifier currents for phase b and phase c can be obtained by multiplying the corresponding switching function with the rectifier dc link current i_{rect} . Thus the rectifier phase a input current is obtained by substituting equations (9) and (15) in (14) and is given below.

$$i_{ar} = A_1 \cos \omega_s t \left[I_{dc} + \sqrt{2} I_{rect} \cos(2\omega_{out} t + \phi) \right] \quad (16)$$

Substituting equations (10), (11) and (12) in (16),

$$\begin{aligned}
 i_{ar} = & \sqrt{2}A_1I_{dc} \cos(\omega_s t + \phi_s) + \\
 & \frac{1}{\sqrt{2}} A_1 I_{rect} \cos((2\omega_{out} t + \omega_s) t + \phi) + \\
 & \frac{1}{\sqrt{2}} A_1 I_{rect} \cos((2\omega_{out} t - \omega_s) t + \phi)
 \end{aligned}
 \tag{11}$$

MATLAB/Simulink model of induction motor is shown in Fig. 3

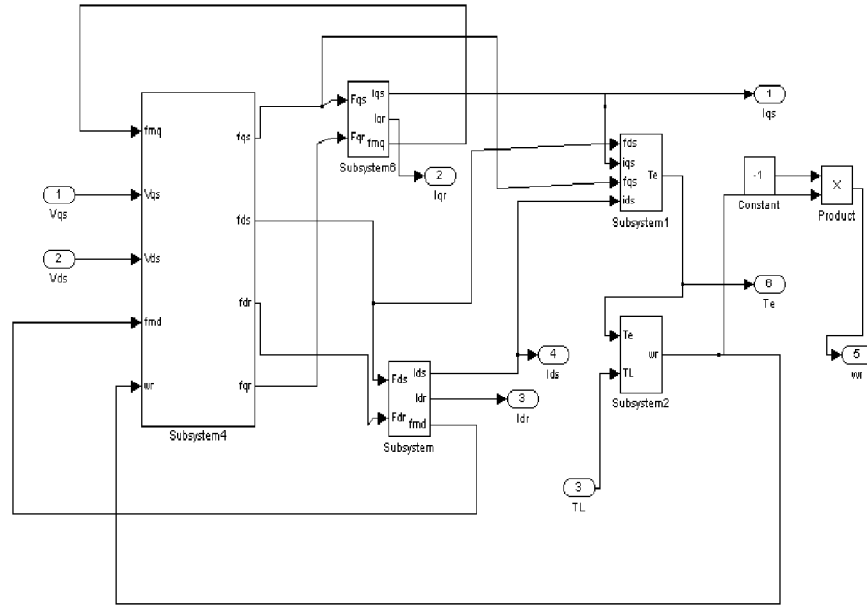


Figure 3

Thus the model is proved through MATLAB/Simulink simulation.

6. SIMULATION OF VFD

Table 1
Induction motor parameters

Rated Power	10 kW
Voltage Rating	415 V
Rated Current	15A
Resistance of stator, R _s	4.9 Ω
Resistance of rotor, R _r	3.63 Ω
Leakage Inductance of stator L _l	10 mH
Leakage Inductance of rotor, L _l	10 mH
Mutual (Magnetizing) Inductance, L _m	20 mH
Pairs of Poles, P	4
Operating Frequency of motor, f _o	10 Hz to 50 Hz
Rated Speed rad/sec	314 r/s

6.1. Simulation of VFD with choke in the input side

The simulink model of the VFD with choke in the input side is shown in Fig.7. Simulation was carried on 10kW induction motor. Motor unbalance is considered by connecting an inductor 0.13mH in series with one of the phases. This creates an approximate motor current unbalance of 3.2%. As the load torque was considered constant, the motor current imbalance also remained constant throughout the simulation. The drive operating frequency is 40Hz. The motor currents were measured and are $I_a=15.37A$, $I_b=15.71A$ and $I_c=15.21A$. The value of the choke connected in the supply side is chosen by trial and error method and is equal to $5\mu H$.

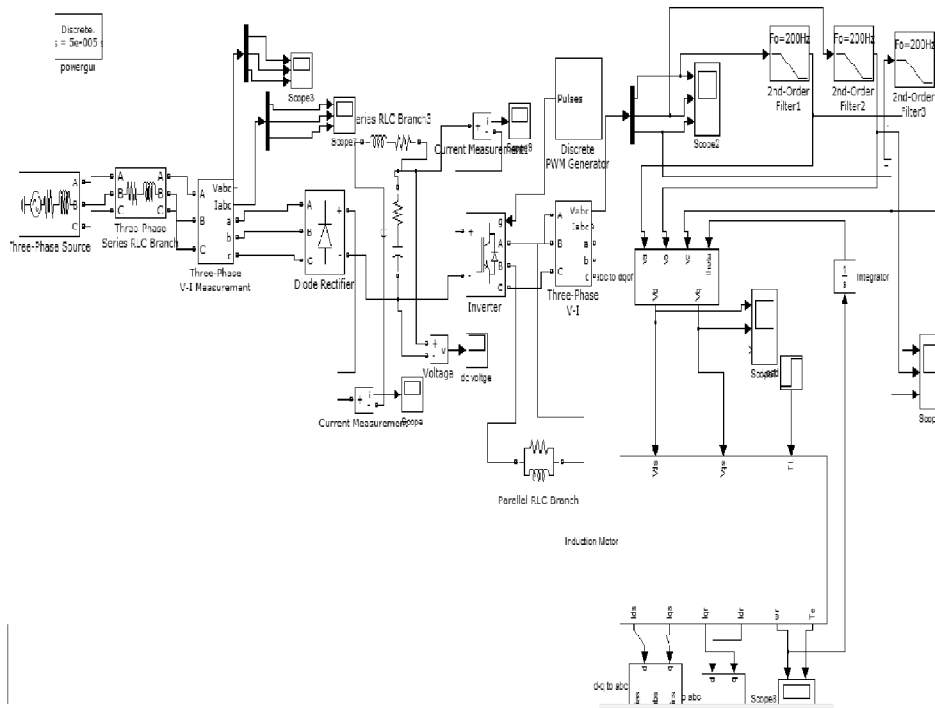


Figure 7

The FFT analysis of supply current is shown in Fig. 9.

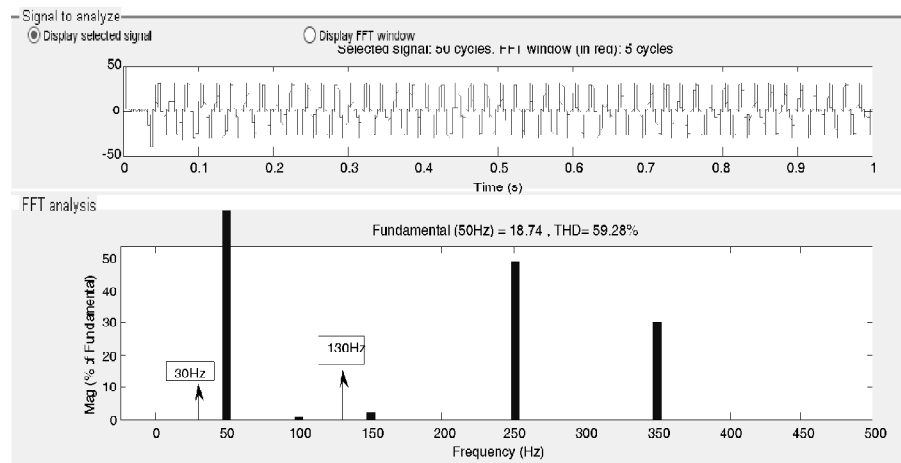


Figure 9

The Total Harmonic Distortion is found to be 59.28%. For an inverter operating frequency of $f_{out} = 40\text{Hz}$, Interharmonics occur at frequencies 30Hz and at 130Hz i.e. at $(2f_{out} \pm f_s)$. f_s is the supply frequency. The Interharmonic magnitudes are found out and tabulated along with 5th and 7th harmonic components and are shown in Table 2.

Table 2

<i>Harmonic/Interharmonic frequency in Hz</i>	<i>Magnitude as percentage of the fundamental</i>
30	0.43
130	0.42
250	49.5
350	29.7

The supply voltage THD is also measured and is shown in Fig. 10.

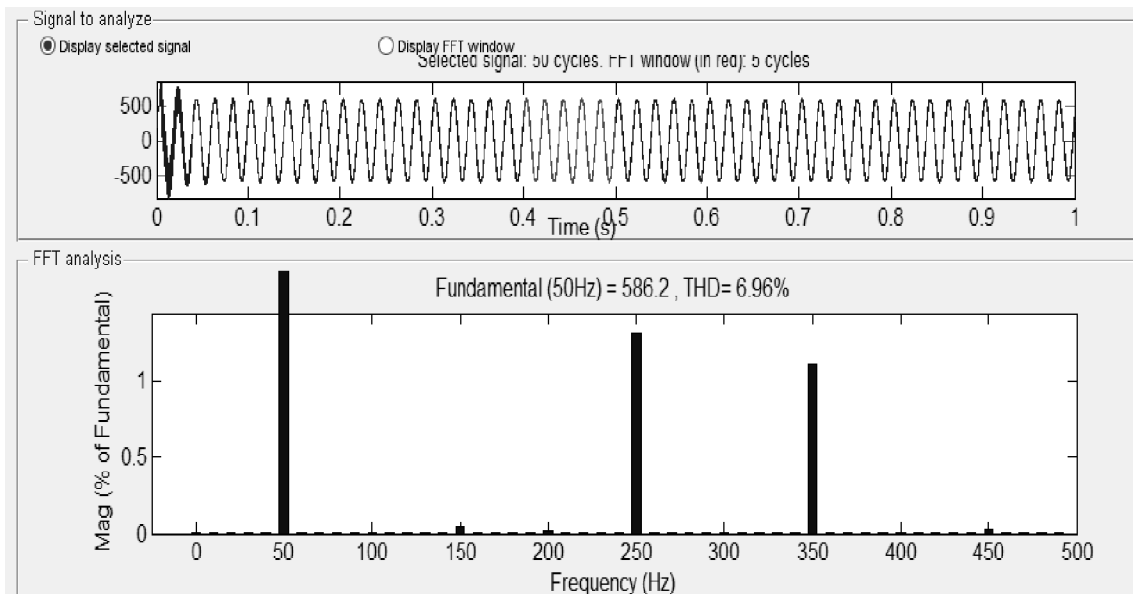


Figure 10

Supply voltage harmonic is found to be 6.96%. But according to IEEE standard, the voltage harmonic should not exceed 5%.

According to the analysis in section 2, for an output frequency of 40Hz, the distortion current amplitude is higher at 80Hz i.e. at $2f_{out}$. The distortion current magnitude is about 58.4% of the fundamental magnitude. Its magnitude increases with the drive operating frequency.

The output of the inverter was filtered using a second order tuned filter and is fed to the induction motor. The FFT analysis of the inverter output voltage is given in Fig. 12.

The motor input voltage has a THD of 2.80% which within the permissible limit given in IEEE standard.

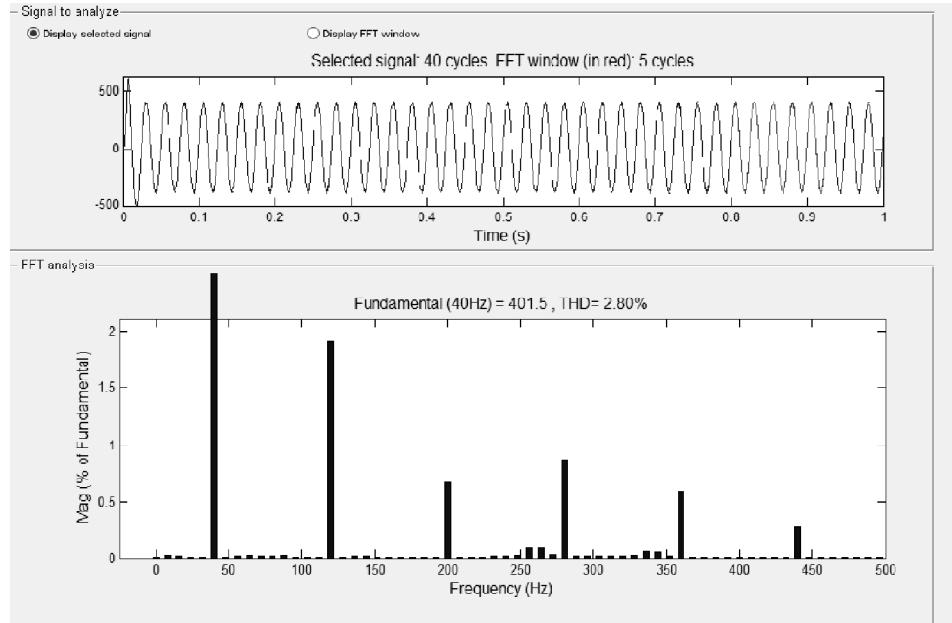


Figure 12

6.2. Simulation of VFD with low pass filter in the input side

Simulation was carried out in an induction motor of the parameters as given in section 4.1. In this low pass filter, the single tuned filter is designed to trap 5th harmonic and is shown in Fig. 14.

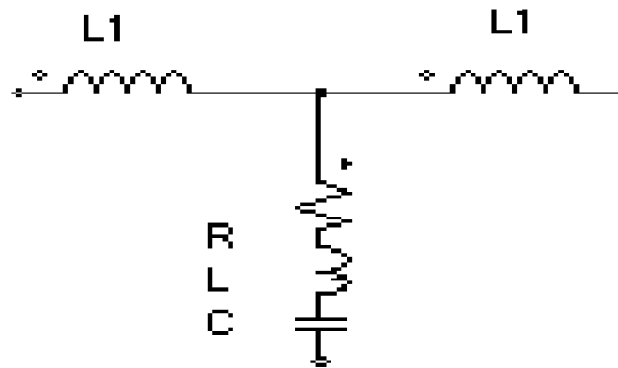


Figure 14

The design equations for the single tuned filter tuned for 5th harmonic is shown below.

A suitable value for Q_c is chosen and corresponding X_c is calculated using

$$X_c = \frac{kV^2}{Q_c} \quad (30)$$

where Q_c is the capacity of the capacitor in kVAr and kV is the voltage rating of the capacitor.

The value of the reactor is calculated using

$$X_L = \frac{X_c}{n^2} \tag{31}$$

Where n is the order of the harmonic. Then the characteristic reactance is calculated using

$$X_n = \sqrt{X_L X_c} \tag{32}$$

Then the value of the reactor resistance is calculated for a specified quality factor Q using

$$R = \frac{X_n}{Q} \tag{33}$$

Quality factor of the coil ranges from 30 to 50. Using these equations the parameters of the single tuned filter are calculated as C=1.256μF, L=0.13H and R=1.014Ω. The value of L1 is found using trial and error procedure and is equal to 10μH. The Simulink model of the VFD with low pass filter in the input side is shown in Fig. 15.

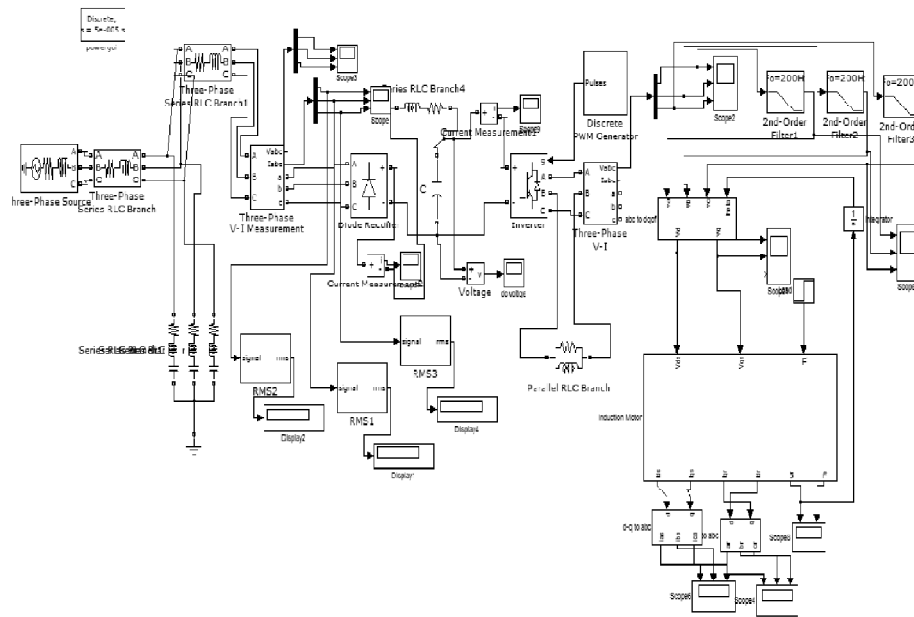


Figure 15

For a drive operating frequency of 40Hz, The input current spectrum are shown in Fig.16 .The magnitude of the input currents are $I_a=13.65A$, $I_b=13.65A$ and $I_c=13.66A$.

The Total Harmonic Distortion is found to be 33.49%. The Interharmonic and harmonic magnitudes are tabulated.

Table 3

Harmonic/Interharmonic frequency in Hz	Magnitude as percentage of the fundamental
30	0.05
130	0.04
250	27.54
350	13.28

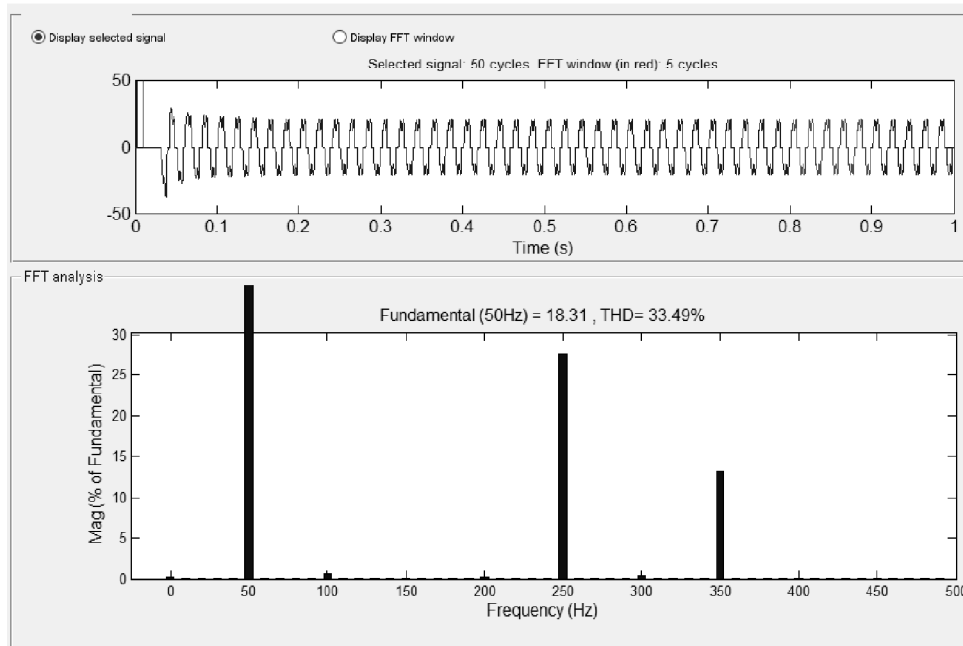


Figure 16

The harmonic and Interharmonic magnitudes are less when compared to a system with choke alone as a filter. The supply voltage THD is calculated using FFT and is shown in Fig. 18.

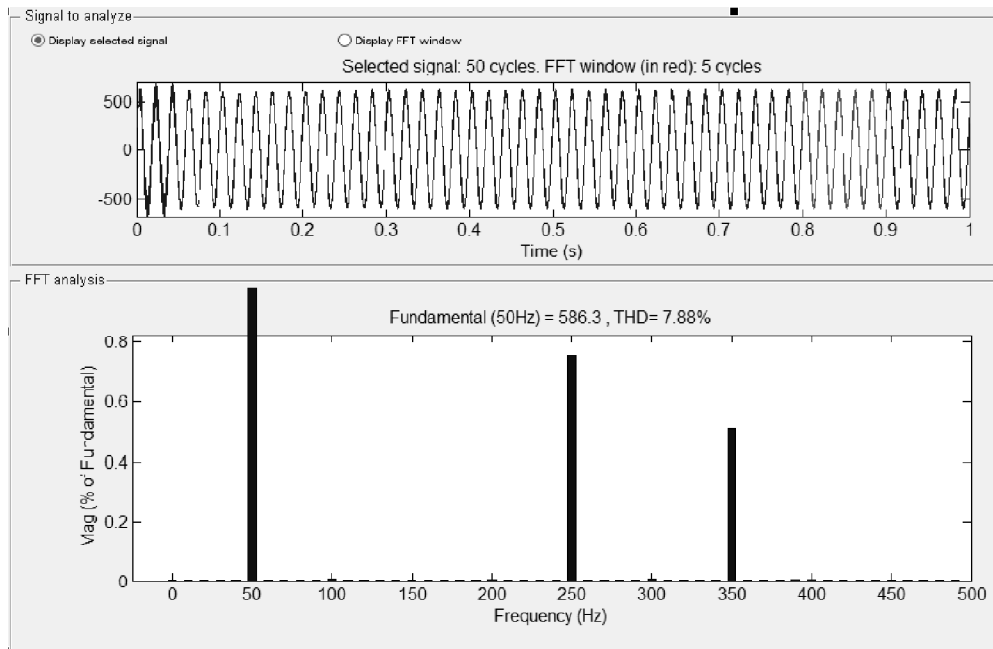


Figure 18

But the supply voltage THD is more in the system with low pass filter. Here it is found to be 7.88% whereas in the case of a system with choke, it is found to be 6.96%.

The distortion current magnitude is about 5.24% of the fundamental magnitude which is much lesser than that with choke alone as filter.

The output of the inverter was filtered using a second order tuned filter and is fed to the induction motor. The FFT analysis of the inverter output voltage is given in Fig. 20.

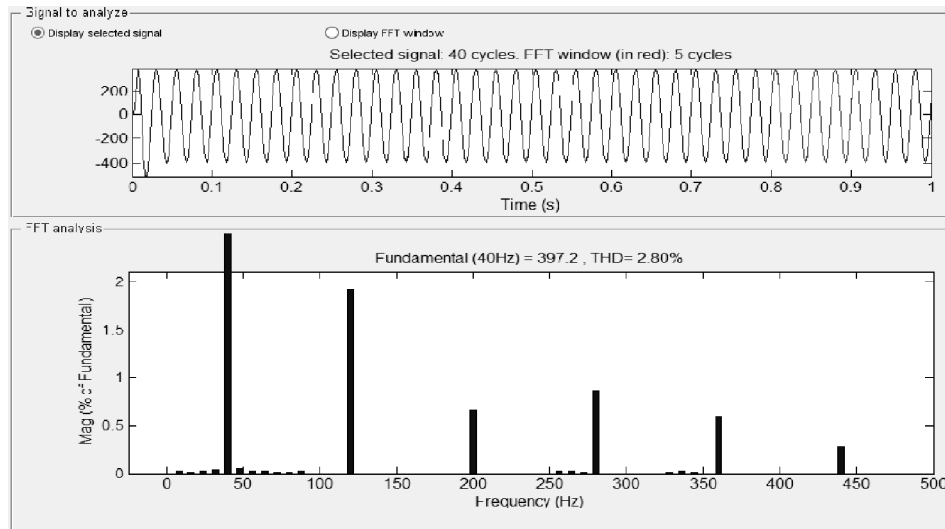


Figure 20

The motor voltage THD is the same and is equal to 2.80%.

6.3. Simulation of VFD with Shunt Active Filter(SAF) in the input side

When choke alone is connected in the input side of VFD, THD of input current is found to be 59.29% and the supply voltage THD is 6.96%. When low pass filter is connected in the input side of VFD, the input current harmonics is 33.49% and supply voltage THD is 7.88%. To reduce the supply current THD, a SAF is designed and connected in the input side of VFD and the input side performance is analysed.

The block diagram of SAF is shown in Fig. 22.

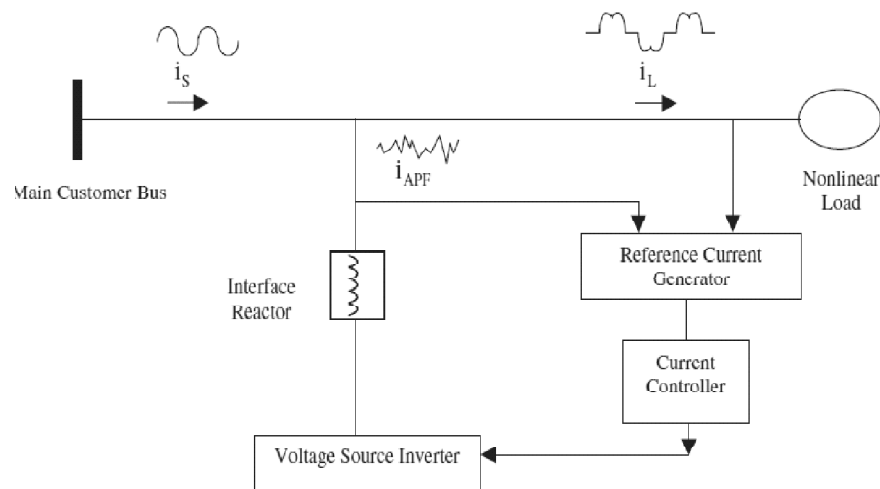


Figure 22

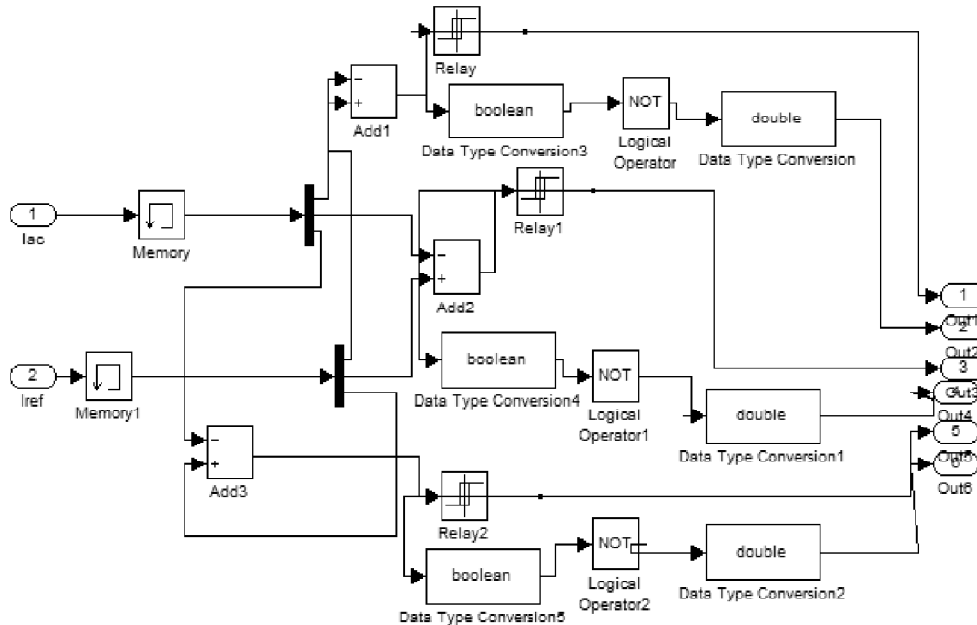


Figure 23

A voltage source inverter is used in the SAF. A SAF is generally employed to eliminate harmonics in the load current. SAF injects a current which is equal but opposite to that of the harmonic current at the point of coupling. The SAF injects i_{sh} into the line such that $i_{sh} = -i_{harm}$ (harmonic current). Synchronous reference frame theory is used for the reference current generation. In synchronous reference frame theory, the three phase currents i_a , i_b and i_c are transformed from three phase reference frame to two phase stationary reference frame currents i_α and i_β .

$$\begin{bmatrix} i_\alpha \\ i_\beta \end{bmatrix} = \sqrt{\frac{2}{3}} \begin{bmatrix} 1 & -1/2 & -1/2 \\ 0 & \sqrt{3}/2 & -\sqrt{3}/2 \end{bmatrix} \begin{bmatrix} i_{La} \\ i_{Lb} \\ i_{Lc} \end{bmatrix} \tag{34}$$

The two phase current quantities i_α and i_β of stationary α - β axes are converted into quantities i_d and i_q in the synchronous or rotating reference frame i.e. d-q axes by the following equation.

$$\begin{bmatrix} i_d \\ i_q \end{bmatrix} = \begin{bmatrix} \sin(\theta) & -\cos(\theta) \\ \cos(\theta) & \sin(\theta) \end{bmatrix} \begin{bmatrix} i_\alpha \\ i_\beta \end{bmatrix} \tag{35}$$

The DC quantities and all other harmonics are transformed to non DC quantities using a low pass filter

$$\begin{bmatrix} i_d \\ i_q \end{bmatrix} = \begin{bmatrix} \bar{i}_d & + & i_d \\ \bar{i}_q & + & i_q \end{bmatrix} \tag{36}$$

The reference currents in $\alpha - \beta$ axes are calculated using the following expression.

$$\begin{bmatrix} i_{\alpha-ref} \\ i_{\beta-ref} \end{bmatrix} = \begin{bmatrix} \sin(\theta) & -\cos(\theta) \\ \cos(\theta) & \sin(\theta) \end{bmatrix}^{-1} \begin{bmatrix} i_d + i_{dc} \\ i_q \end{bmatrix} \quad (37)$$

The compensating currents in a,b,c axes are calculated using the following equation.

$$\begin{bmatrix} i_{a-ref} \\ i_{b-ref} \\ i_{c-ref} \end{bmatrix} = \sqrt{\frac{2}{3}} \begin{bmatrix} 1 & 0 \\ -\frac{1}{2} & \frac{\sqrt{3}}{2} \\ -\frac{1}{2} & -\frac{\sqrt{3}}{2} \end{bmatrix} \begin{bmatrix} i_{\alpha-ref} \\ i_{\beta-ref} \end{bmatrix} \quad (38)$$

Hysteresis current control is implemented whose Simulink diagram is shown in fig 23.

The dc link voltage is controlled using a PI controller. The transfer function of a closed loop control of dc link is

$$\frac{\Delta V_{dc}}{\Delta ref} = \frac{K_p K I_s \cos \phi \sqrt{3} / C V_{dc} . s + K_p K I_s \cos \phi \sqrt{3} / T_i C V_{dc}}{s^2 + K_p K I_s \cos \phi \sqrt{3} / C V_{dc} . s + K_p K I_s \cos \phi \sqrt{3} T_i C V_{dc}} \quad (39)$$

The simulink model of the VFD with SAFin the input side is shown in Fig. 24.

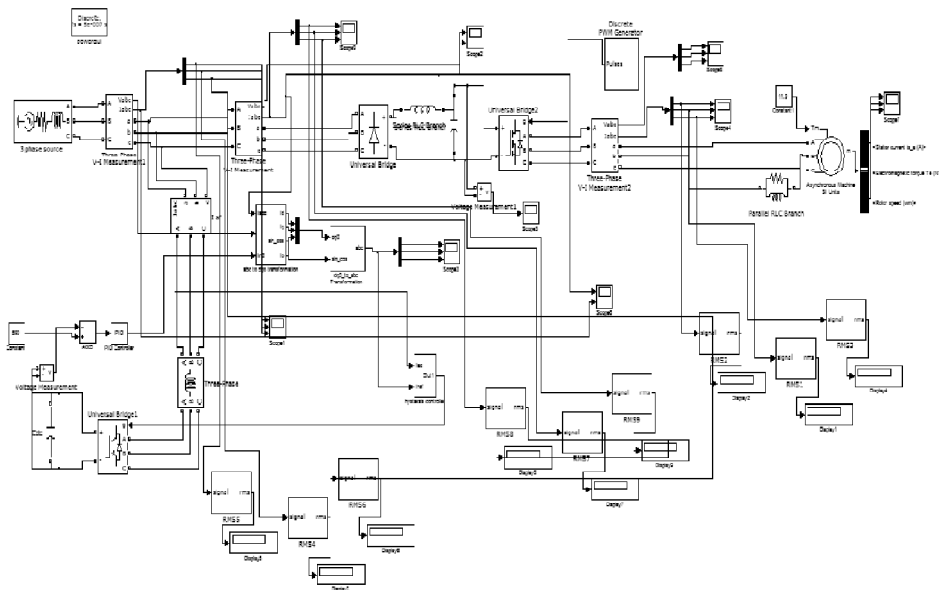


Figure 24

The magnitude of the input currents are $I_a=15.93A$, $I_b=14A$ and $I_c=15.98A$.

The source current spectrum waveform shown in Fig. 26.

The current spectrum shows a THD of 5.77%. But here, the harmonic magnitudes around fundamental frequency have increased. The Interharmonic and harmonic magnitudes are tabulated

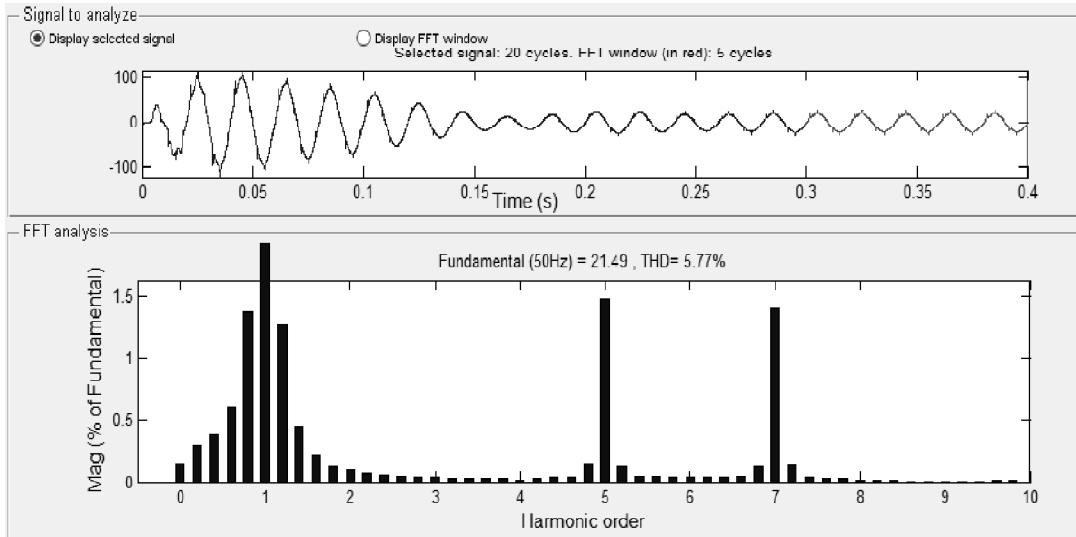


Figure 26

Table 4

Harmonic/Interharmonic frequency in Hz	Magnitude as percentage of the fundamental
30	0.15
130	0.01
250	1.48
350	1.4

The THD and harmonic magnitudes are considerably less when compared to a system with choke and low pass filter. But the Interharmonic magnitude at 30Hz is increased. The supply voltage THD is calculated using FFT and is shown in Fig. 27.

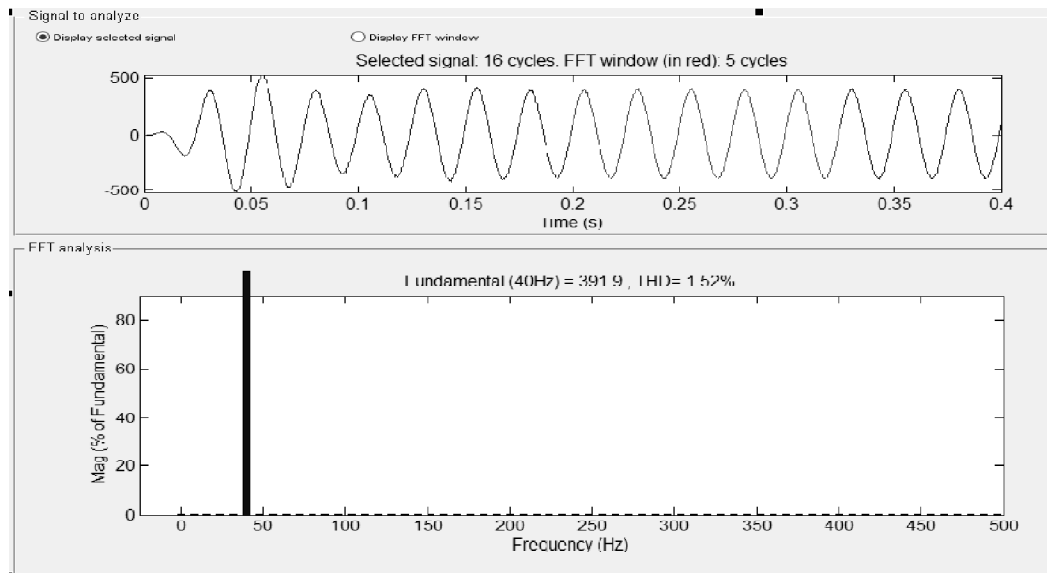


Figure 27

THD of supply voltage is much less when compared to the system with passive filters. The motor voltage spectrum is shown in fig. 28

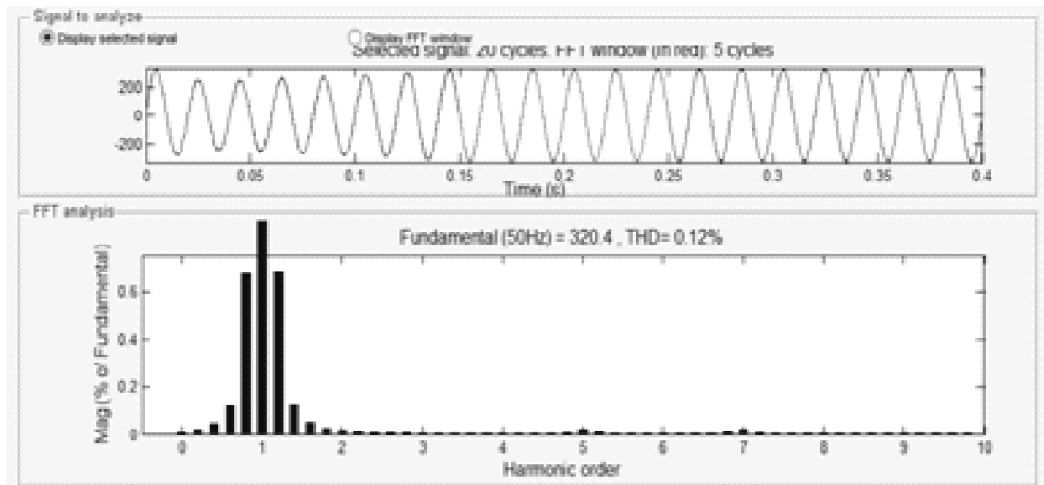


Figure 28

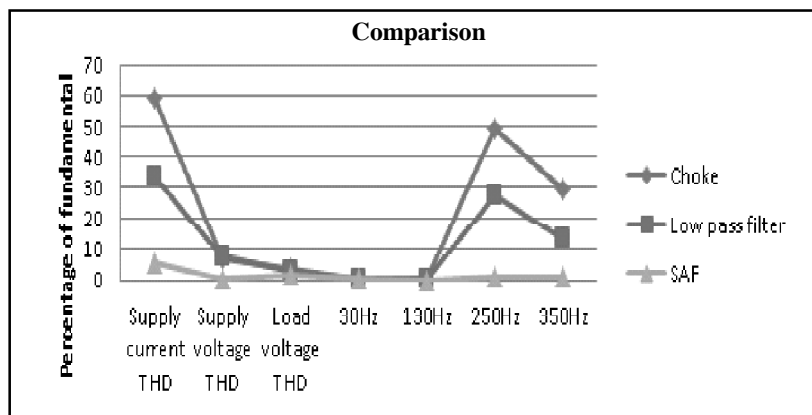
The motor voltage THD is found to be equal to 1.52%.

The various values obtained as a percentage of fundamental by connecting an inductor in series with the supply, by connecting a low pass filter in the supply side and by connecting a SAF in the supply side are compared and are shown in Table 5.

Table 5

Parameters	Choke	Low pass filter	SAF
Supply current THD	59.29	33.49	3.82
Supply voltage THD	6.99	7.88	0.12
Load voltage THD	3.87	2.8	1.52
30Hz	0.43	0.05	0.15
130Hz	0.42	0.04	0.01
250Hz	49.5	27.54	0.81
350Hz	29.7	13.28	0.74

The comparison chart shown in Fig.29 clearly indicates that SAF gives comparatively better results. The supply voltage and supply current THD obtained are within the values specified in IEEE 519 standard.



7. CONCLUSION

Solution to mitigate harmonics and Interharmonics in the input of VFD has been proposed in this work. First an inductor is used in the supply side that reduced harmonics in the input current and its THD is equal to 59.29%. Then a low pass filter was designed and connected in the input side gave a THD of 33.49%. Finally a SAF was designed and connected in the input side gave a THD of 5.77%. The harmonic and Interharmonic magnitudes are also considerably reduced when SAF is employed. Thus SAF has been proven to be an effective method for mitigating harmonics and Interharmonics in a VFD.

REFERENCES

- [1] CEI/IEC 1000-2-1, 'Electromagnetic Compatibility', Part 2: Environment, Section 1: Description of the environment*/ Electromagnetic environment for low-frequency conducted disturbances and signaling in public power supply systems, 1st ed., 1990.
- [2] Erich W. Günter, "Interharmonics in Power Systems", IEEE Power Eng. Soc. Summer Meeting Vol. 2, July 2001, pp813-817.
- [3] A. Testa, "Issues Related to Interharmonics", IEEE Power Eng. Soc. General Meeting, Vol.2 July 2003, pp1198-1203.
- [4] IEEE Interharmonic Task Force, "Interharmonics: theory and modeling," IEEE Trans. Power Del., vol. 22, no. 4, pp. 2355–2348, Oct.2007.
- [5] J.Arrillaga, N.R.Watson, and S.Chen, Power System Quality Assessment. New York: Wiley, 2000.
- [6] M.H.J.Bollen, Understanding Power Quality Problems: Voltage Sags and Interruptions . New York: IEEE Press, 2001.
- [7] R.C.Dugan, S.Santoso, and M.F.McGranaghan, Electric Power Systems Quality , 2nd ed. New York: McGraw-Hill, 2004.
- [8] A. M. Munoz, Ed.,, Power Quality: Mitigation Technologies in a Distributed Environment . London, U.K.: Springer, 2007, Ed..
- [9] A. Testa, M. Akram, R. Burch, G. Carpinelli, G. Chang, V. Dinavahi, C. Hatziaioniu, W. Grady, E. Gunther, M. Halpinetal., "Interharmonics: theory and modeling," IEEE Trans. Power Del., vol. 22, no. 4, pp. 2335– 2348, Oct. 2007.
- [10] Seyed Reza HadianAmrei and Dian GuoXu, "A New Study On Harmonics And Interharmonics Reduction With Frequency Selective Closed-Loop Control In Vsi Inverters", IEEE Vehicle Power and Propulsion Conference (VPPC), September 3-5, 2008, Harbin, China.
- [11] Ravi Kumar Jujjuvarapu & B. Basavaraja, "Modelling And Estimating Voltage And Current Harmonics Of Variable Speed Drives (VSD)", International Journal of Power System Operation and Energy Management ISSN (PRINT): 2231 – 4407, Volume-1, Issue-4, 2012
- [12] Duro Basic, "Input Current Interharmonics of Variable-Speed Drives due to Motor Current Imbalance," IEEE Trans. Power Del. Vol.25, no. 4, Oct.2010.
- [13] F. De Rosa, R. Langella, A. Sollazzo, and A. Testa, "On the inter harmonic components generated by adjustable speed drives," IEEE Trans. Power Del., vol. 20, no. 4, pp. 2535–2543, Oct. 2005.